Jül-Conf-45 D2-3

I C A N S - V

MEETING OF THE INTERNATIONAL COLLABORATION ON

ADVANCED NEUTRON SOURCES

June 22-26, 1981

Relative Intensities and Time Structure of Thermal Neutron Leakage from Various Moderator-Decoupler Systems for a Spallation Neutron Source

G.S. Bauer, J.P. Delahaye**, H. Spitzer*, A.D. Taylor+ and K.Werner**

* Institut für Festkörperforschung, Kernforschungsanlage Jülich
D-5170 Jülich, West Germany

** Division PS, CERN, CH-1200 Geneva

+ Rutherford and Appleton Laboratories, Chilton, Didcot, OX11 OQX, UK

Abstract

Measurements were performed using the short bursts of 800 MeV protons at the CERN booster synchrotron to study the effect of surface structure, decoupling and poisoning of moderators on the intensity and time structure of a spallation neutron source. It was found that grooves in the moderator surface can enhance the neutron leakage by almost a factor 2 for poisoned and decoupled moderators as well as for non-decoupled ones, with only a minor effect on the time structure. Also, it could be shown that Cd with a decoupling energy of only 0.4 eV can replace B_4C with a decoupling energy of 3 eV with almost no effect on the time structure. This makes it much easier to provide decoupler cooling in a real design.

1. Introduction

In recent years there has been a growing interest in pulsed neutron sources based on the spallation reaction as induced by energetic particles impinging on heavy nuclei (see e.g. J.M. Carpenter, 1977). These sources are accelerator driven and can therefore be designed with a high degree of flexibility with respect to time structure and neutron spectral distribution. Similar to the case of a fission reactor, the neutrons are originally generated with a kinetic energy around 1 MeV and have to be slowed down to energies below 1 eV to be used in the condensed matter research for which such sources are designed. In these sources moderators are placed close to the target, and to increase their efficiency, they are surrounded by a fast neutron reflector. The task in designing such a system is threefold:

(1) Provide as intense a neutron beam as is possible

(2) Provide neutron bursts of very short duration

(3) Find a design which is technically feasible with respect to space requirements and heat removal.

Generally the figure of merit for a pulsed neutron source is taken as

$$M = \frac{I(E)}{(\Delta t(E))^2} , \qquad (1)$$

where I is the neutron current emerging from the moderator surface and Δt is the width of the pulse of neutrons of energy E.

To achieve short pulses, the moderator is surrounded by a layer of material called decoupler (see Fig. 1), which ideally is transparent for fast neutrons but opaque for thermal and slow neutrons. If a 1/v-absorber, such as boron-10 is used, one has a high degree of flexibility in choosing the effective decoupling energy by adjusting the thickness of the boron layer (Taylor, 1979). 2.3 MeV of energy is, however, released by the absorption process and appears as kinetic energy of the recoil fragments (Li-7 and He-4). This energy is deposited locally, making such a decoupler difficult to cool. It is therefore desireable to use an (n,γ) absorber such as cadmium or gadolinium so that the reaction energy may be dissipated over an extended volume. Similar considerations hold for the heterogeneous poison (Fig. 1) embedded in the moderator to avoid too long a time spread due to neutrons emerging from deep inside the moderator.

On the other hand, it had been found (Bauer et al, 1980) that the integrated leakage of neutrons from a hydrogeneous moderator can be considerably increased by not using a flat surface moderator but working a series of grooves into the surface. These have the effect of extracting neutrons from the higher flux inside the moderator.

It was the purpose of the present experiments, to study the effect of using low energy decouplers (like Cd, with a decoupling energy of 450 meV) and grooved surface moderators on the intensity and time structure of the extracted thermal neutron beam.

2. Experimental setup and -procedure

The measurements were performed at the end of the measurement line of the 800 MeV CERN booster synchrotron (PSB). This synchrotron is part of the CERN ring system (Fig. 2). It takes protons from the 50 MeV linac and, after acceleration to 800 MeV delivers them to the 28 GeV PS-ring (PSR) which in turn can serve the Super Proton Synchrotron (SPS), Intersecting Storage Rings (ISR) or the 28 GeV experimental areas. The cycle time of these systems being an integral multiple of the cycle time of the booster (0.8 sec), there are spare cycles available at the booster where parasitic use of accelerated particles is possible. Depending on the mode of operation of the other facilities, the separation between these parasitic pulses may be up to 2.4 sec. The maximum number of protons that can be accelerated in the four rings of the PSB is 2×10^{13}. In each ring the pulse train of 5 pulses is 0.6 μs long and the four pulse trains can be combined to give one pulse train of 20 pulses and 2.4 μs long (Fig. 3). If pulses from less than four rings are used, there results an even shorter proton burst. In most of our measurements only ring 3 was used with 5×10^{11} protons accelerated. This was to minimize dead time effects in the detector.

The spallation target was located in front of the PSB beam dump. It consisted of solid lead, 400 mm long, 100 mm high and 600 mm wide. It was designed to simulate the geometry of the rotating target conceived for the high power spallation source presently under study in West Germany. The moderators used were 20 cm long blocks of polyethylene placed above the front end of the target. They were surrounded on three sides by 20 cm of beryllium to act as a fast neutron reflector. Only the moderators were changed in the course of the experiment. The target-moderator-reflector arrangement was mounted on a cart which could be remotely moved out of the path of the proton beam to make the PSB-beam dump available for normal use (Fig. 4). A stationary shield of 0.5 to 1 m thickness of iron and lead was put in place to avoid excessive radiation levels in the adjacent PSR-tunnel and to reduce the fast neutron return from the walls around the experimental setup.

A pyrolytic graphite crystal (mosaic 0.4° FWHM) was used to select neutrons of well-defined energies from the thermal spectrum emerging from the moderator and to diffract them onto a well shielded detector located at 5.19 m from the moderator (Fig. 5). A Soller type collimator, 5 cm high and with an aperture of 0.75° was placed between the moderator and the analyser crystal. The scattered beam was limited by a B_4C-slit 2 mm wide and 40 mm high (6 mm wide and 90 mm high for measurement N* of Table 1) at 342 cm from the detector which was an 8 atm He-3 detector of 12 mm diameter and 30 cm active length. As imposed by the spatial constraints, the analyzer was set at $2\,\theta_A = 90°$. It was mounted on a turntable which could be controlled remotely to move the analyser out of the beam for background measurements. A second motor provided a rocking adjustment about the $2\,\theta_A = 90°$ position.

The protons were monitored by an intensity transformer which delivered a signal between 0 and 5 volts whose height was proportional to the number of protons in a pulse train. This signal was digitized by an ADC and a pulse height analysis performed in the multichannel analyser. In this way the proton burst intensity distribution was measured and the total number of protons on the target was proportional to the first moment of this distribution. Examples of measured proton distributions are shown in Fig. 6. Each time a proton pulse train hit the target, a time circuit was triggered and the number of neutrons arriving

at the detector were analyzed as a function of time. With the energy defined by the scattering angle of the analyser crystal ($2\theta_A = 90°$), this yielded the time distributions of the neutrons of energies corresponding to the various orders of the crystal reflections.

3. Measurements and Data Evaluation

The moderators used are shown in Fig. 7. They were made of polyethylene and in general were 20 cm long and 10 cm high (18 cm long and 8 cm high for the case of the B_4C-decoupler). The "flat" moderators were 75 mm thick with the possibility of placing a heterogeneous poison (a 0.025 mm thick sheet of Gd) at 25 mm under the viewed surface. In the case of the "grooved" moderators, the front part was machined as shown in Fig. 7a to contain 15 mm deep grooves with 50 % of the material removed. They could be heterogeneously poisoned like the flat ones. Decouplers consisted either of 0.5 mm cadmium sheet surrounding the moderator and leaving a 100 x 100 mm^2 channel towards the analyser open or of 10 mm thick boron-loaded plastic (decoupling energy $\sim$ 3 eV) of the same shape (see Fig. 8). The combinations examined are given in Table 1 and are labelled according to the following notation: grooved moderators are marked by an asterix, the poison used is set in paranthesis and the decoupler is used for the characterization with N standing for no decoupler.

For each combination a run with the crystal analyser in place and one without analyser was taken. An example of the raw data is shown in Fig. 9 for run B_4C. The various orders of reflexions are superimposed on a strongly time-dependent continuum. This is caused by fast neutrons penetrating the shielding and getting slowed down somewhere near the detector. The minimum visible at about 400 μs corresponds to the Cd-resonance. (The shield of the detector had an inner layer of cadmium). For the first 200 μs the detector was saturated.

It was found that this continuous background was not only caused by fast neutrons emerging from the target but there seems to have been a strong contribution from beam spills at other positions along the beam line. This was confirmed by removing the target from the beam and measuring the background with the beam going into the beam dump. For this reason it was not possible to correct for the background by normalizing to the number of protons recorded.

However, it was found that, except in the region of the Bragg peaks, the ratio between signal and background was completely flat. This is examplified in Fig. 10, where this ratio is given in a logarithmic representation for the B_4C-run. The same is true, if the background measurements for the various runs are compared. It was therefore concluded that the continuum part of the data is independent of the moderator configuration used. Since the proton energy, target and shielding remained the same for all runs, the continuum in the region of the Cd-resonance (644 μs ÷ 720 μs), was used to normalize the spectral and background measurements.

Examples of spectra corrected for background in this way are shown in Figs. 11 through 15. From Figs. 11a, b and c the effect of decoupling and poisoning on the line width is clearly visible. Note that the plots are not normalized. A comparison between Figs. 12a and 12b shows that the grooves have no significant effect on the time structure. However, the relative intensities between the

reflections corresponding to different energies indicate that the grooved moderator produces a considerably softer neutron spectrum than does the flat one.

From Fig. 13, which is the same as Fig. 9 but in logarithmic representation, it is obvious that the background cannot be described by one single exponential function, so the following procedure was adopted to examine the individual peaks of the spectra more closely:

- For the time window corresponding to the peak under consideration, an exponential function is fitted to the background run.
- The intensity of this exponential is then scaled at the Cd-resonance region (see above) and this fitted function is removed from the data. (Fig. 14 shows these data for the B_4C-run)
- From the net intensities thus obtained the following parameters were derived:

  normalized peak height, P

  normalized peak intensity, I

  "width" of peak, $W = \frac{I}{P}$

  standard deviation σ in μs (second moment of the intensity distribution)

Normalization of P and I was done with respect to the number of protons recorded. For the standard deviation only 99 % of the peak intensity was included to avoid domination of the integral by statistical errors in the long time tail of the peak. The results are given in Table 2 through 5.

The intensity data for the N^* case have not been included in all listings because these measurements were taken with a strongly detuned analyser crystal which resulted in low count rates and relatively poor statistical accuracy. The experimental setup has been changed after measuring the N^* case (different slits, fully aligned analyser crystal). More extensive studies on undecoupled and unpoisoned moderators will be reported separately (Bauer et al, 1981).

In order to evaluate the N and N^* measurements, which is not as straightforward as for the decoupled moderators due to overlap between pulses, the procedure followed was:

- The background was determined as before
- Starting with the 00 12 reflection, an exponential decay with two decay constants was fitted to the difference (signal minus background).
- This contribution was extrapolated to longer times and subtracted from the following peak.
- The result was used for fitting an exponential decay to the following peak etc.

In this way, the net intensities of the various peaks were obtained, which were then used to derive the same quantities as for decoupled moderators. An example of the peaks obtained after correction for overlap and the corresponding fit data is shown in Fig. 15. While there was an obvious need for two decay constants, it was necessary for the 006-reflection to keep the amplitude (A_1) of

one of the decay modes fixed in order to obtain results which are consistent with the neighbouring peaks. This amplitude was derived from a smooth curve drawn through the amplitude obtained for the other peaks as shown in Fig. 16, where the open circles indicate the amplitudes that resulted from the first fit and the full symbols give the data obtained with A_1 selected to lie on the curve. Also shown in Fig. 16 are the decay contants associated with the various amplitudes.

A comparison of the integrated intensities relative to those obtained for the B_4C(Gd) case is given in Fig. 17. It can be seen that the Cd(Gd) case is very similar to the B_4C(Gd) case. The effect of the grooves in the surface on the intensity in the Cd(Gd) case is a gain by a factor of 1.8 above 10 meV and even more below 10 meV (indicating, as noted before, that the grooved moderator gives a much softer spectrum than the flat one). Similarly, in the unpoisoned case the grooves lead to a considerable intensity gain (see also Bauer et al, 1981).

The "width" as determined by the ratio of the integrated intensity to peak height is affected by the spectrometer resolution (see below) only through the reduction of the peak height, whereas the second moments, in addition to being sensitive to peak broadening, are also affected by the somewhat arbitrary choice of the integration limits.

On the other hand, the shape of the peaks, which is not well represented by either one of the two quantities may become very important if a weak reflection has to be separated from an intense one by time-of-flight in an actual neutron spectrometer. For this reason we give in Table 7 a summary of the contours of the various peaks measured. For each peak the measured width at 50 %, 30 %, 10 %, 3 % and 1 % of the peak intensity are given (excluding the N and N^* cases).

From these data it can be seen that some pulse shape degradation takes place with the grooved moderator surface, especially at longer neutron wavelengths, but around 1 Å the pulse shape is not significantly affected.

From the semi-logarithmic plots of Fig. 14 it can be seen that the trailing edge of most of the peaks can be described fairly well by one or two exponential decay modes. Since, if measured not too close to the peak, the decay constants are fairly independent of the time resolution of the arrangement, we give a list of decay constants obtained for the various moderators in Table 6. If two decay constants are given, the first one is the dominant one at long times whereas the second one is measured in the region close to the peak and hence may be somewhat less certain. For the N and N^* cases, two decay constants are given for all reflections. Their respective amplitudes in the N-case can be found in Fig. 15, from which it is obvious that the two contributions are of similar magnitude.

4. Discussion

4.1 Time resolution of the experimental arrangement

Owing to the space and equipment available to perform the present measurements, it was not possible to set up a backscattering time focussed arrangement which would have minimized resolution effects on the measured data. The resolution of the configuration used can be estimated as follows: Due to the fact that a 2 mm wide slit and a 12 mm Ø detector, 3.42 m apart determined the angular resolution of the detector leg, this contribution to the total resolution is

negligible. The wavelength (and time-) resolution of the arrangement is therefore determined by the collimator in front of the analyser crystal ($\Delta\theta_1 = 0.75°$ FWHM) and the mosaic width of this crystal ($\Delta\theta_2 = 0.4°$ FWHM). With the direction of the outgoing beam strictly fixed, the crystal acts as a mirror, i.e. each orientation of its mosaic blocks will only reflect neutrons of a well defined wavelength and incident angle onto the detector. In this case the transmission of the system is given by the product of the transmissions of the components.

$$T(\theta) = T_1(\theta) \times T_2(\theta)$$

Approximating both, T_1 and T_2 by Gaussians whose standard deviations are equal to the standard deviation of the true resolution functions, we have

$$\text{for the crystal} \quad T_2 = \exp\left\{-\frac{\theta^2}{2\sigma_2{}^2}\right\}$$

$$\text{with} \quad \sigma_2 = \frac{\Delta\theta_2}{2\sqrt{2\ln 2}} = 2.96 \cdot 10^{-3}\text{rad}$$

$$\text{for the collimator} \quad T_1 = \exp\left\{-\frac{\theta^2}{2\sigma_1{}^2}\right\}$$

$$\text{with} \quad \sigma_1 = \sqrt{\frac{\Delta\theta_1{}^2}{6}} = 5.34 \cdot 10^{-3}\text{rad}$$

(the transmission function of the collimator is actually a triangle)

This yields

$$\frac{1}{\sigma^2} = \frac{1}{\sigma_1{}^2} + \frac{1}{\sigma_2{}^2} = 1.49 \cdot 10^5 \text{ rad}^{-2}$$

$$\sigma = 2.59 \cdot 10^{-3} \text{ rad} \qquad (2)$$

From the Bragg condition it follows

$$\frac{\Delta\lambda}{\lambda} = (\text{ctg } \theta_A) \cdot \sigma = 2.59 \cdot 10^{-3} \text{ (standard deviation)} \qquad (3)$$

with $\theta_A = 45°$.

In order to apply a correction for time resolution to quantities other than the standard deviation, such as the FWHM, the shape of the measured curve has to be known. In some cases (such as the higher order reflections in the unpoisoned moderator cases as shown in Fig. 14) a steep rise followed by an exponential decay is a fairly good description. In this case (exponentially decaying function with decay time τ) we have

for the full width at half maximum

$$(\text{FWHM})_{\text{exp}} = \tau \cdot \ln 2 \qquad (4)$$

and for the standard deviation

$$\sigma_{exp} = \tau \cdot \sqrt{2} \tag{5}$$

The resolution at FWHM then is

$$\left(\frac{\Delta t}{t}\right)^{exp}_{1/2} = \sigma \frac{\ln 2}{\sqrt{2}} = 1.27 \cdot 10^{-3} \tag{6}$$

For the case of a poisoned moderator and especially for lower order reflections where the rise time and the decay time are of the same order of magnitude, such a description is not sufficient. In these cases the curves become more symmetrical. If, for the purpose of determining the FWHM, a triangular shape can be assumed, we have

$$(FWHM)_{tri} = \sigma \cdot \sqrt{2} \tag{7}$$

or

$$\left(\frac{\Delta t}{t}\right)^{tri}_{1/2} = 3.66 \cdot 10^{-3} \tag{8}$$

Finally, if a Gaussian shape of the peak would have to be assumed, one would get

$$(FWHM)_{gauss} = \sigma \cdot 2\sqrt{2 \ln 2} \tag{9}$$

or

$$\left(\frac{\Delta t}{t}\right)^{Gauss}_{1/2} = 6.10 \cdot 10^{-3} \tag{10}$$

The FWHM's given in Table 7 have been calculated, using equ (8) throughout.

4.2 Comparison of configurations

4.2.1 Effect of grooves in the surface

As noted before, a grooved moderator surface results in an increase of thermal neutron leakage (for the case without decoupler, this has been shown indenpendently, (Bauer et al, 1980 and 1981). However, it also affects the pulse shape. From Fig. 18, where we show the 004-reflections for the various configurations as an example, it can be seen by comparing plots c to e and d to f respectively, that both the rise and the fall times are affected by the grooves. The rise occurs at an earlier time for the grooved moderators in both cases. This effect is more pronounced in the unpoisoned than in the poisoned case. This cannot be explained by actual flight path difference since, for the case of the unpoisoned moderator, the shift corresponds to 1 % of the total flight time which would mean a flight path difference of almost 6 cm. It appears therefore that in the grooved moderator the neutrons start leaking out of the surface earlier than without the grooves. Also, a small feature seems to appear before the actual rise in the case of the grooved moderators. On the other hand, somewhat surprisingly, the decay times for the grooved moderators seem to be shorter in the undecoupled and Cd-decoupled cases than for a moderator without grooves, at least in the low energy range (cf. Table 6).

4.2.2 Effect of Gd-poison

The addition of the Gd-poison has a significant effect on the pulse width through the decay time but - within the experimental resolution - not on the rise time. The overall effect on the integrated intensity being quite dramatic (Fig. 17), the peak intensity (Table 3) is only reduced by a factor between 0.75 (002-reflection) and 0.93 (006-reflection) for the Cd-decoupled moderator and seems to be virtually unaffected for the higher decoupling energy of the B_4C (the apparent slight increase is probably within the limits of the experimental accuracy).

4.2.3 Effect of Cd-decoupler vs. B_4C-decoupler

Using a Cd-decoupler which has a relatively low decoupling energy of only 0.4 eV rather than a B_4C-decoupler (the effective decoupling energy of the B_4C used was $\sim$ 3 eV), results only in marginal pulse broadening, especially for the poisoned moderator. Since, in a practical design, B_4C would be hard to use because of the high energy deposition density of the α-particles produced, Cd seems to be a viable alternative as a decoupler. Here the energy of the γ-ray produced is carried much further away from the decoupler.

5. Conclusions

The present measurements, which were mainly aiming at giving an idea as to what the penalty in intensity (peak height and integrated intensity) would be by going from an undecoupled moderator system as proposed for the German spallation neutron source project with 500 μs duration of the proton pulses to a decoupled one with short pulses show, that the reduction of the peak intensity caused by the decoupler and poison is a modest one, the effect on integrated intensity of course being quite dramatic.

Using an improved time resolution spectrometer, a study of moderator optimisation and target-moderator geometry is necessary to assess the possible benefits of working grooves into the moderator surface for a pulsed spallation source. Such a program is presetly in progress at Los Alamos (Russell et al 1981)

Acknowledgement

We are very much indepted to Dr. G.L. Munday, leader of the CERN PS-Division, for granting the permission to do these experiments on very short terms and in an unburocratic way. The personal engagement and continuing support by Dr. K.H. Reich, leader of the PS-Booster-group, and his staff and their readiness in fulfilling our needs and demands in every possible way, were of invaluable help to our crew. The help of Mr. B. Boland with part of the measurements and of Dr. H. Conrad with part of the data evaluation is greatly appreciated. Also, we would like to thank Mr. E. Hanning, Mr. H. Crämer and Mr. H. Möller for their technical assistance.

References

Bauer G.S., Conrad H.M., Friedrich K., Milleret G. and Spitzer H. (1981)
"Measurement of Time Structure and Thermal Neutron Spectra for Various Target-Moderator-Reflector Configurations of an Intensity-Modulated Spallation Neutron Source", this volume

Bauer G.S., Grünhagen K. und Spitzer H. (1980)
"Einige Voruntersuchungen zu wasserstoffhaltigen Moderatoren für eine Spallations-Neutronenquelle", SNQ-report, part III A2, unpublished

Carpenter J.M. (1977)
"Pulsed Spallation Neutron Sources for Slow Neutron Scattering"
Nucl. int. Math., 145 91-113

Russell G.J., Meier M.M., Gilmore J.S., Prael R.E., Robinson H. and Taylor A.D. (1981)
"Measurement of Spallation Target-Moderator Neutronies at the Weapons Neutron Research Facility"
in Proc. ICANS IV meeting, report KENS-2 pp. 210-241

Taylor A.D. (1980)
"Neutron Transport from Targets to Moderators"
in Proc. Meeting on Targets for Neutron Beam Spallation Sources (G.S. Bauer et al), Jül-Conf. 34, p. 47-76, ISSN 0344-5798

Decoupler	Flat Moderator		Grooved Moderator	
	Poison		Poison	
	none	Gd	none	Gd
B_4C	B_4C	B_4C(Gd)		
Cd	Cd	Cd(Gd)	Cd*	Cd(Gd)*
none	N		N*	

Table 1 Combinations of moderators, decouplers and poison investigated and corresponding abbreviated notations.

Configuration	Reflection					
	00.2	00.4	00.6	00.8	00.10	00.12
B_4C	27.6	145.0	156.1	95.9	33.7	9.7
B_4C(Gd)	17.4	85.5	86.2	53.1	20.0	5.3
Cd	47.8	228.7	242.7	150.8	49.8	9.8
Cd(Gd)	19.1	87.1	88.7	56.9	21.6	6.2
Cd*	96.4	340.3	334.0	207.8	71.4	16.4
Cd(Gd)*	47.8	160.9	150.6	95.0	36.2	10.1
N	180	838	854	405	154	42
N*	-	-	-	-	-	-

Table 2 Normalized integrated intensities of reflection peaks from graphite analyser. Data not corrected for crystal reflectivities and detector efficiency.

Configuration	Reflection					
	00.2	00.4	00.6	00.8	00.10	00.12
B_4C	1.0	5.3	6.0	4.8	2.4	1.1
B_4C(Gd)	0.9	5.7	6.5	5.2	2.7	1.1
Cd	1.6	7.2	7.7	6.3	3.6	1.4
Cd(Gd)	1.0	5.3	5.8	4.9	2.6	1.0
Cd*	3.1	8.9	8.9	7.6	4.4	1.9
Cd(Gd)*	2.3	8.1	8.3	7.0	3.9	1.6
N	2.38	8.5	9.4	7.52	4.02	1.8
N*	-	-	-	-	-	-

Table 3 Normalized heigths of reflection peaks from graphite analyser. Data not corrected for crystal reflectivities and detector efficiency.

Configuration	Reflection					
	00.2	00.4	00.6	00.8	00.10	00.12
B_4C	107	109	104	80	55	34
B_4C(Gd)	75	59	53	41	29	19
Cd	121	127	126	95	54	28
Cd(Gd)	78	66	60	46	34	25
Cd*	126	153	150	110	65	34
Cd(Gd)*	83	79	72	54	37	25
N	313	394	363	218	147	93
N*	235	309	218	(266)	(227)	(191)

Table 4 "Width" of reflection peaks in μs from graphite analyser as obtained from the ratio of integrated intensity to peak height. Values in parentheses for the N* 008, 0010 and 0012 reflections are uncertain due to convergency problems of the fit.

Configuration	Reflection					
	00.2	00.4	00.6	00.8	00.10	00.12
B_4C	65.1	69.1	76.5	66.0	57.7	40.2
B_4C(Gd)	33.1	29.7	27.5	25.8	47.2	38.6
Cd	70.8	77.5	82.0	69.2	52.5	25.2
Cd (Gd)	37.7	32.2	30.6	29.5	38.7	22.6
Cd*	71.0	80.9	86.1	71.2	55.6	35.8
Cd (Gd*)	38.7	38.1	50.0	40.0	38.2	23.5
N	330.8	380.5	378.8	243.4	305.1	245.1
N*	300.0	356.5	185.1	551.9	471.4	258.8
σ^*_{res}	16.6	8.4	5.6	4.2	3.4	2.7

Table 5 Second moments of intensity distribution (μs) in the analyser reflections.

Configuration	Reflection					
	00.2	00.4	00.6	00.8	00.10	00.12
B_4C	70	75	77	75/55	75/25	
B_4C(Gd)	30	30	25	25	15	
Cd	75	85	88	84/60	80/30	
Cd(Gd)	30	30	30	27	20	
Cd*	75	80	80	85	85/30	
Cd(Gd)*	35	35	32	30	20	
N	468/113	577/232	547/155	352/83	455/46	350/20
N*	414/ 51	557/161	258/120	(900/120)	(700/70)	(350/22)

Table 6 Decay times (μs) for the various reflection peaks from the graphite analyser. Data are not corrected for time resolution. Data in parentheses indicate difficulties with the fits.

Configuration	% of Peak Int.	Reflection 00.2	00.4	00.6	00.8	00.10	00.12
B_4C	50	85	85	79	49	25	17
	30	128	135	128	98	59	27
	10	227	220	216	190	174	(120)
	3	326	319	319	302		
	1	418	426	433	(390)		
B_4C(Gd)	50	65	50	45	33	20	15
	30	92	71	63	49	30	21
	10	131	106	99	80	56	46
	3	176	145	128	119	83	
	1	220	200	177	149		
Cd	50	94	103	99	65	29	
	30	147	156	156	115	58	
	10	248	255	255	210	147	
	3	348	358	358	314		
	1	440	468	472			
Cd(Gd)	50	69	57	52	39	25	18
	30	96	79	72	55	38	26
	10	135	117	110	88	61	42
	3	191	150	152	136	90	
	1		213	206	176		
Cd*	50	101	133	128	84	35	18
	30	156	184	177	136	70	27
	10	252	284	284	234	180	112
	3	355	390	(383)	(325)		
	1	454	532				
Cd(Gd)*	50	77	71	64	43	26	18
	30	99	98	85	61	39	27
	10	149	138	121	98	72	49
	3	199	181	167	153	122	
	1	262	248	248			
Wavelength (Å)		4.7	2.4	1.6	1.2	0.95	0.79
time μs		6582	3306	2212	1659	1331	1065
Resolution (μs)		23.5	11.6	7.8	5.8	4.7	3.9

Table 7 Intensity contours (μs) for the various reflections, not corrected for resolution. The resolution at FWHM is given in the bottom line.

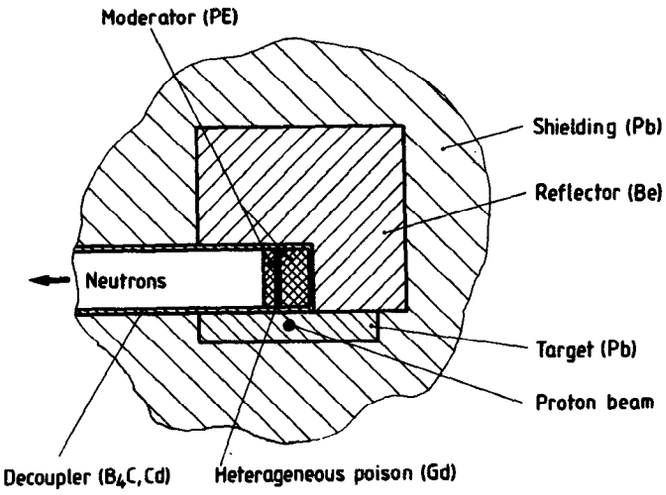

Fig.1
General arrangement of a target-moderator-reflector setup for a pulsed spallation neutron source. The moderator is decoupled from the surrounding materials (target and reflector) by an absorber for thermal neutrons. To improve pulse quality, a heterogeneous poison (absorber) can be used at a certain depth below the surface, from which the neutrons are extracted.

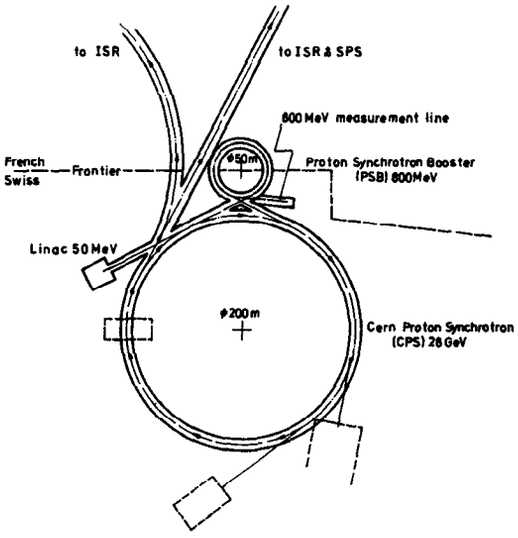

Fig.2
The CERN-PS ring system. The experiments described in this report were performed at the end of the 800 MeV measurement line.

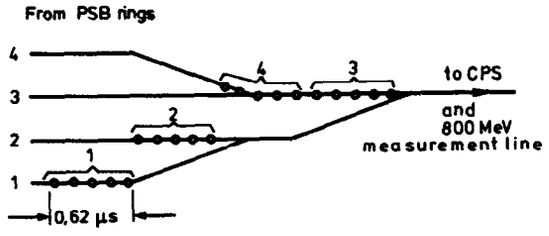

Fig.3
Combination of proton bunches accelerated in the four rings of the PSB to form one 2,6 μs pulse. If only one ring is used, as in the present experiments, the pulse is 0,62 μs long.

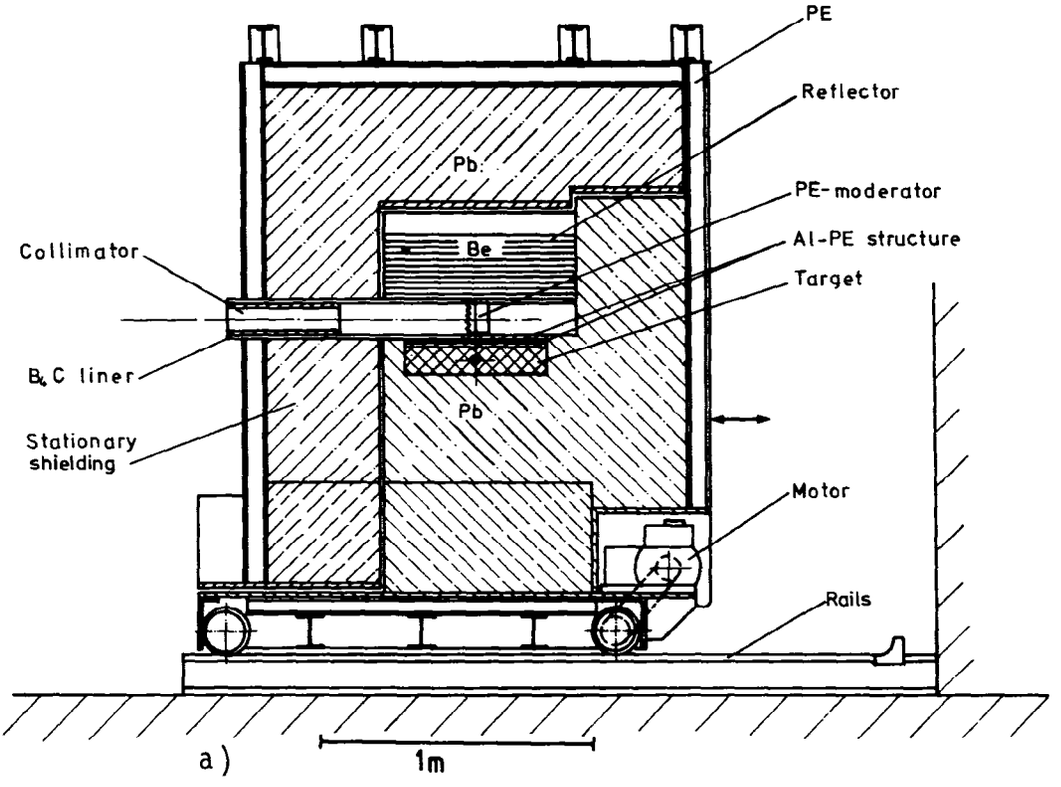

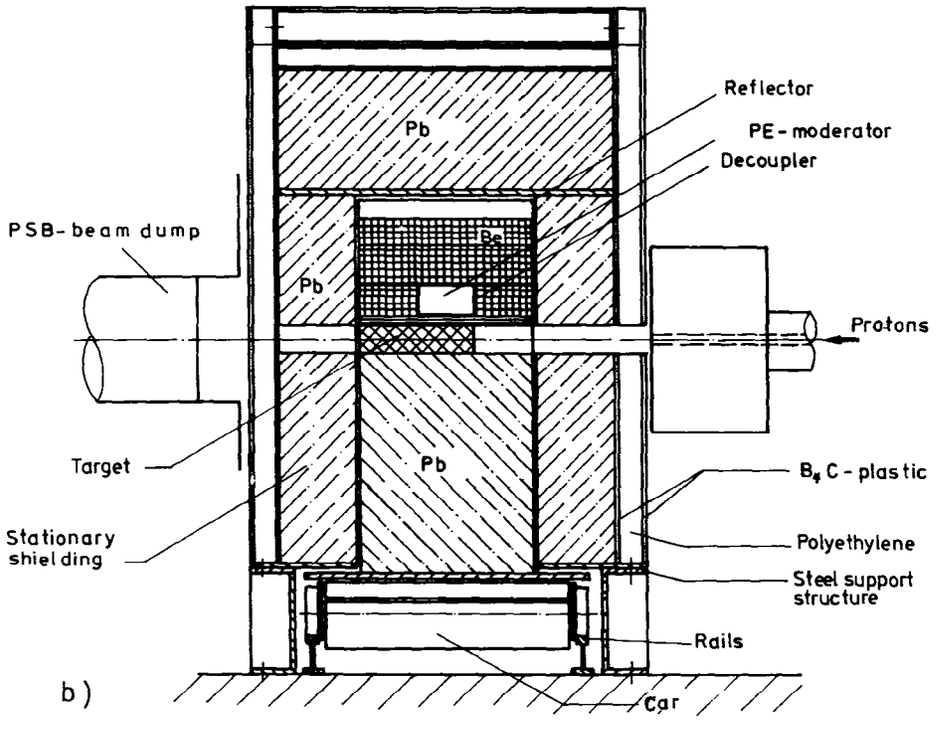

Fig. 4

Mockup of spallation neutron source arrangement used in the experiments.
For easier replacement of target, moderator and reflector part of the arrangement could be moved on a trolley.

a) Elevation perpendicular to the direction of the proton beam.
b) Elevation parallel to the direction of the proton beam.

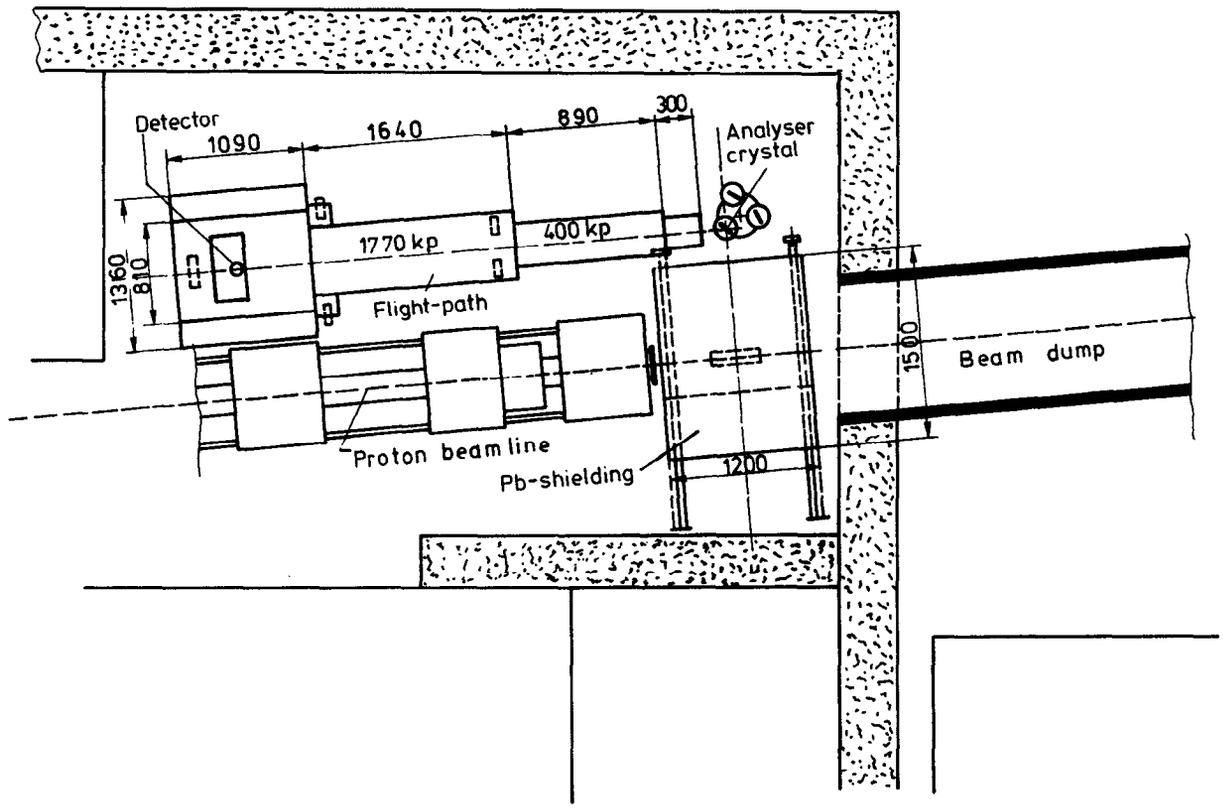

Fig. 5 Plan view of the experimental setup showing the proton beamline, the spallation source mockup, the crystal analyser table and the neutron flight path at the end of the 800 MeV measurement line.

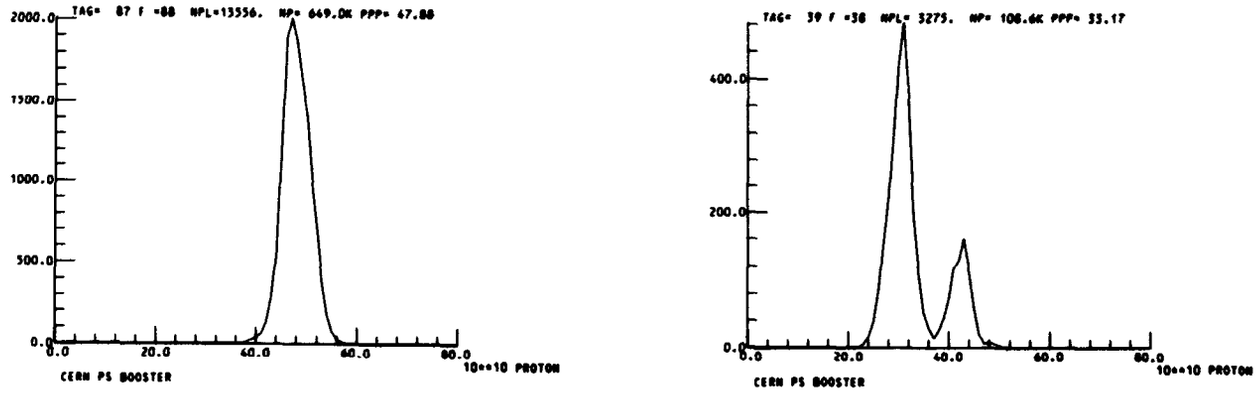

a) b)

Fig. 6 Examples of proton pulse-height spectra, showing one case of fairly constant proton intensity and one case where the number of protons per pulse changed during the experiment as visible from the two distinct peaks in the spectrum.

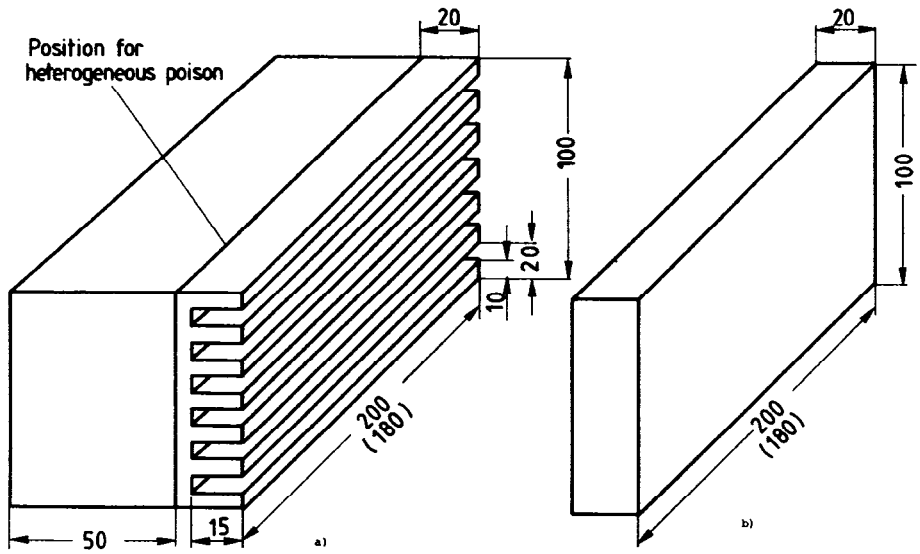

Fig. 7 The moderators (polyethylene). The flat slab of 20 mm thickness could be exchanged for the grooved part of the moderator. Neutrons were extracted at right angles to the grooved surface. If a heterogeneous poison was used, it was placed between the two parts of the moderator.

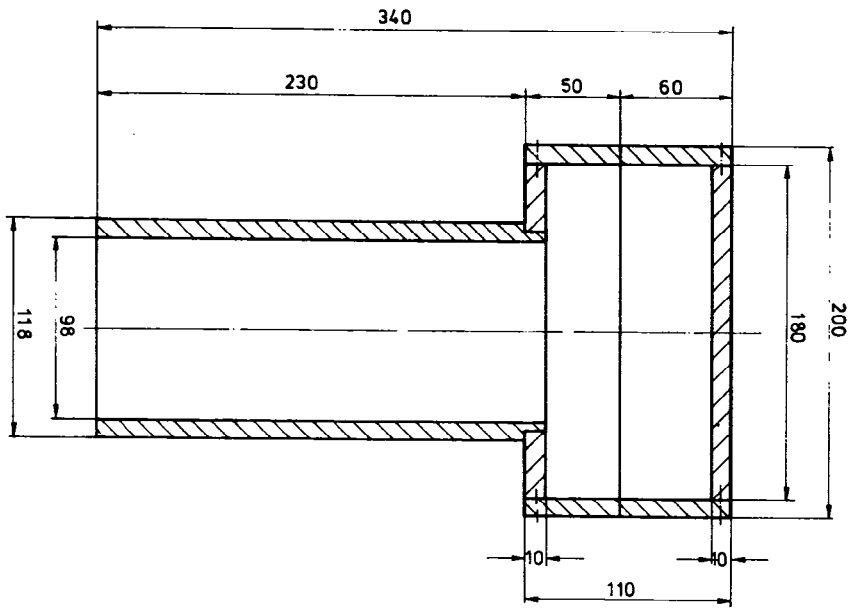

Fig. 8 The B_4C-plastic decoupler used. The B_4C-content was 50% natural B_4C in the material.

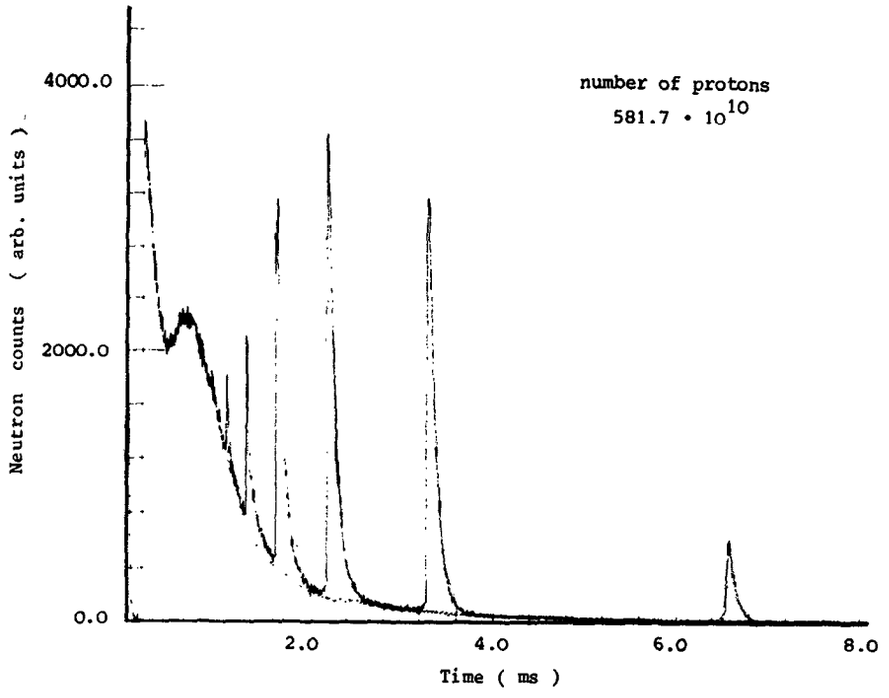

Fig. 9 Neutron spectrum as measured for the flat moderator with B_4C-decoupler. The peaks corresponding to the various orders of reflections from the graphite crystal are superimposed on a strongly time-dependent background. The minimum at about 500 μs corresponds to the Cd-resonance.

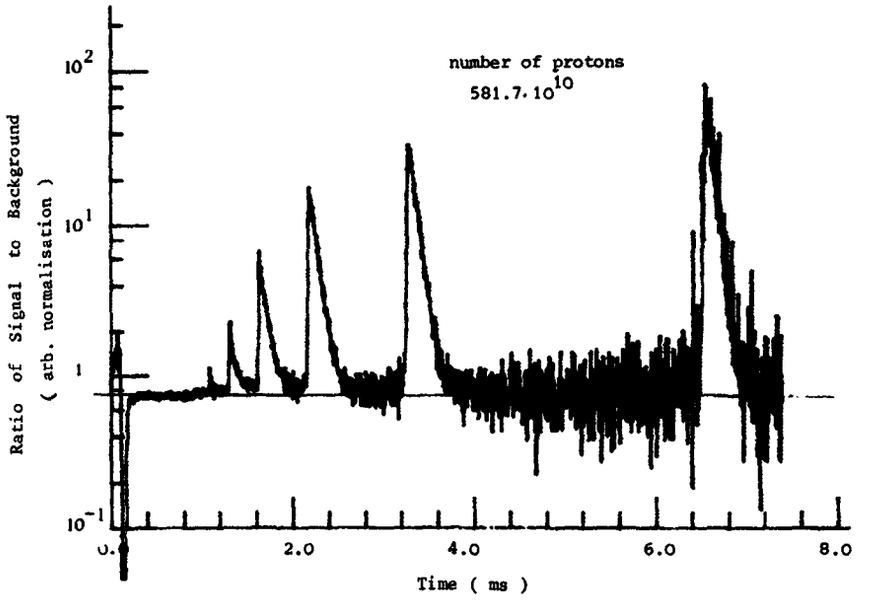

Fig. 10 Logarithmic representation of the ratio between measured data and background measured without analyser for the same measurement as Fig. 9. Apart from the reflection peaks, the ratio is seen to be completely flat.

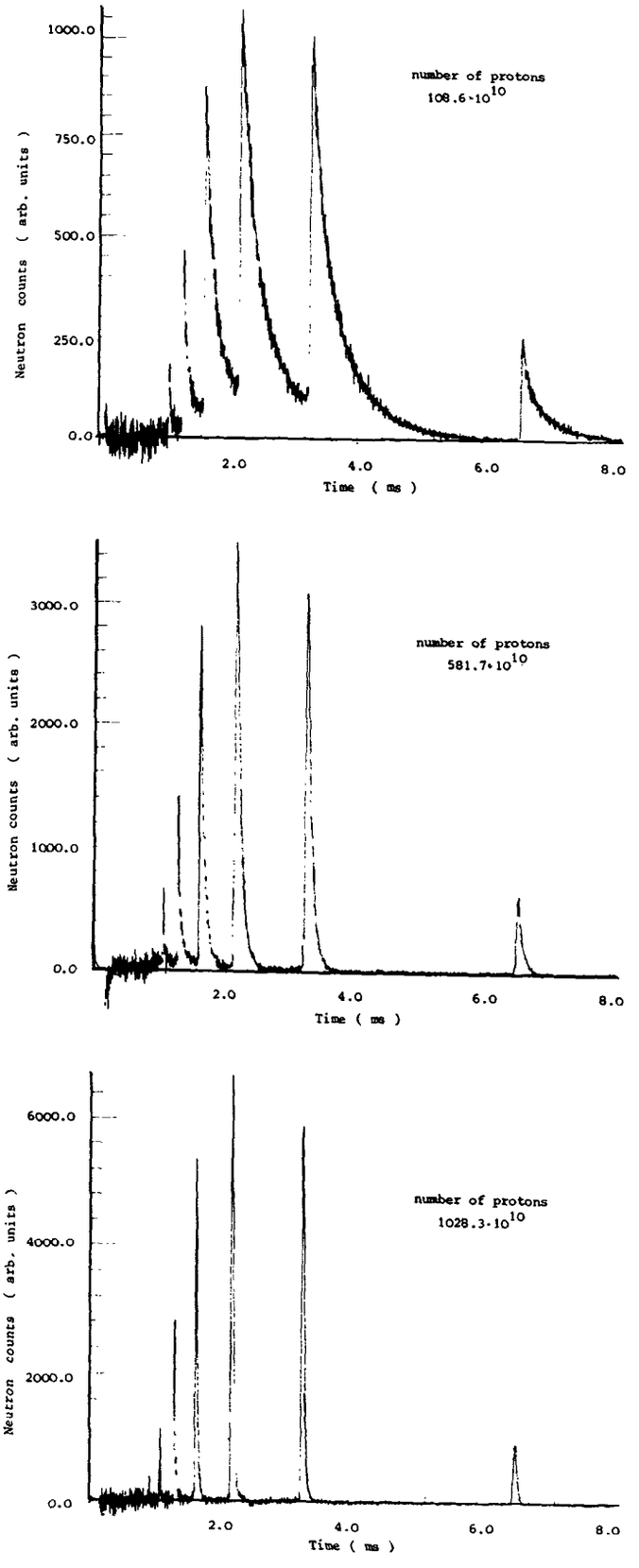

Fig. 11 Effect of decoupler and poison on pulse shape of the crystal reflections (flat moderator surface)

a) no poison, no decoupler

b) no poison, B_4C decoupler

c) Gd-poison, B_4C decoupler

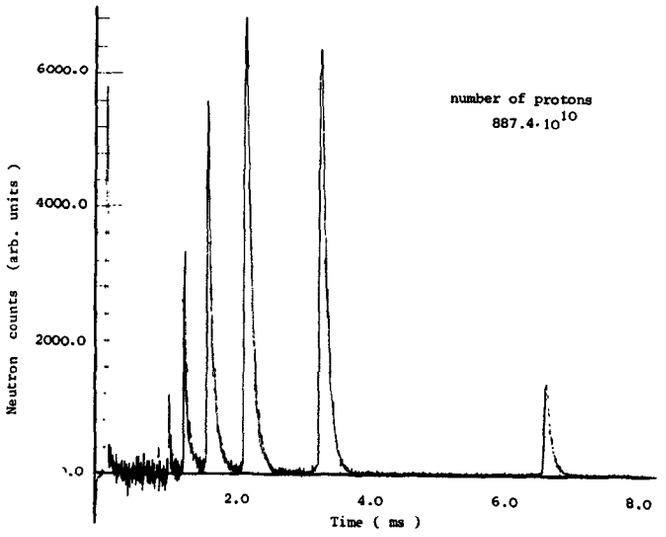

a)

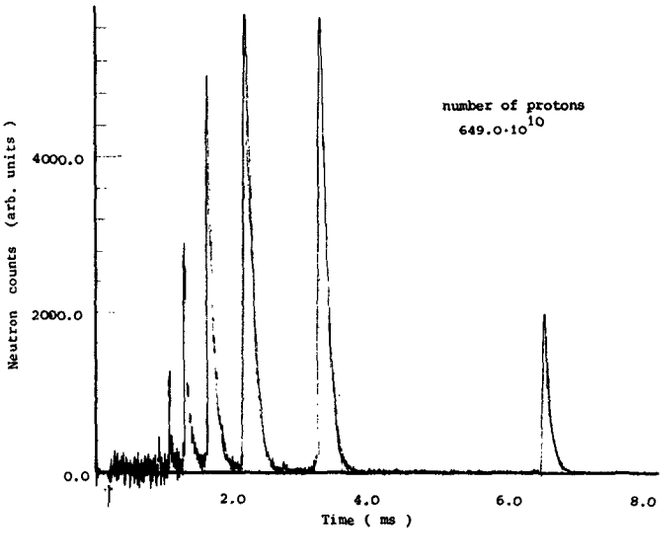

b)

Fig. 12
Comparison of pulse shapes from flat and grooved moderator surface with Cd-decoupler, no poison.
a) flat surface
b) grooved surface

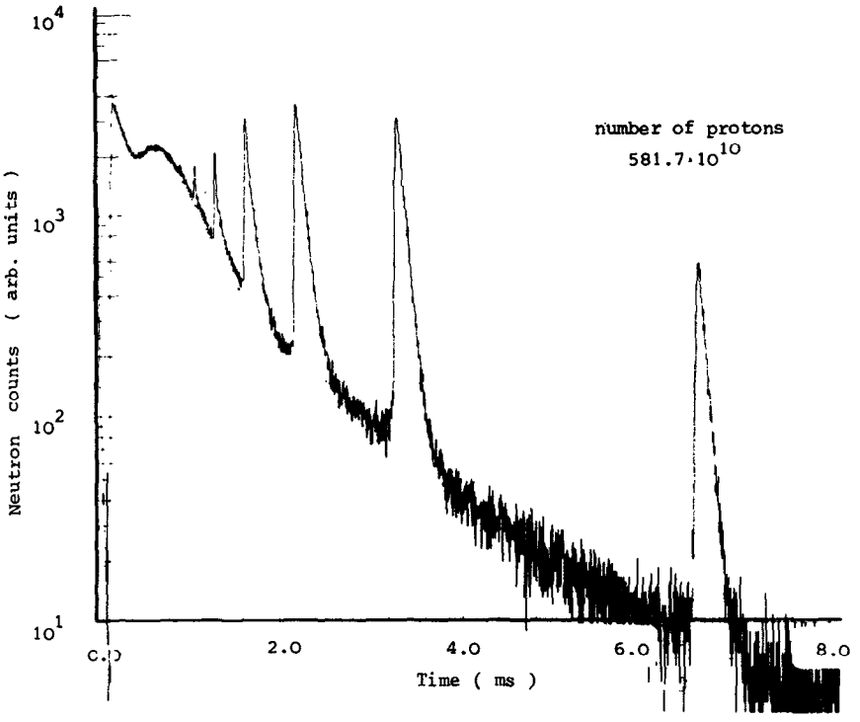

Fig. 13

Logarithmic representation of measured raw data (same as Fig. 9) showing, that the background cannot be described by a single exponential decay function.

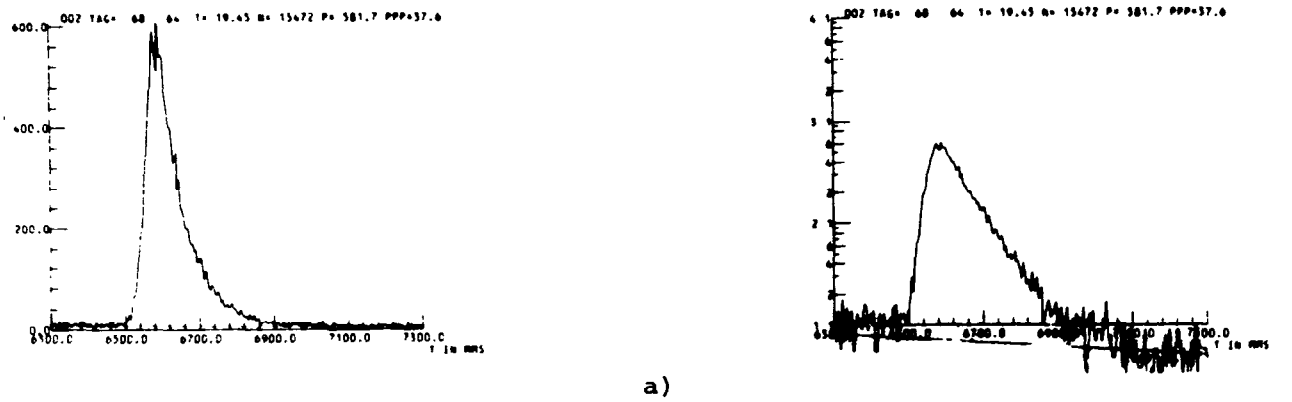

a)

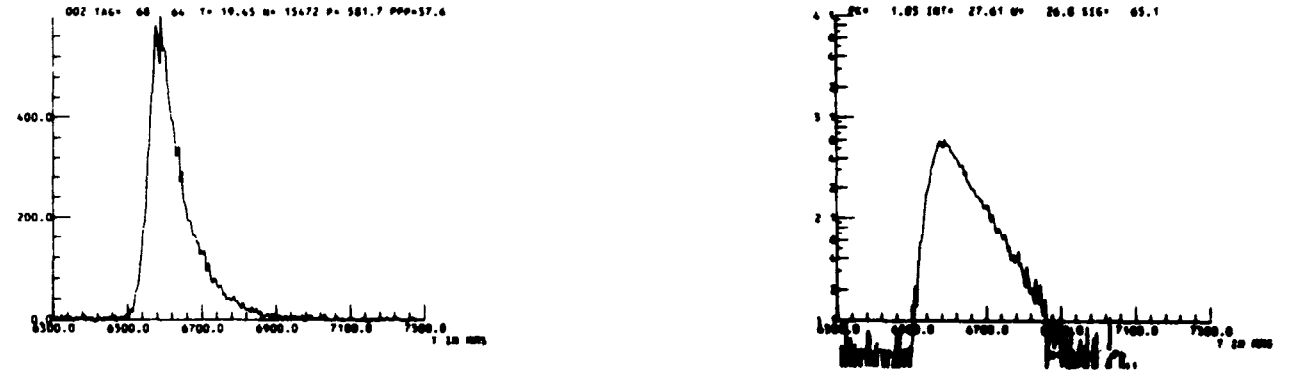

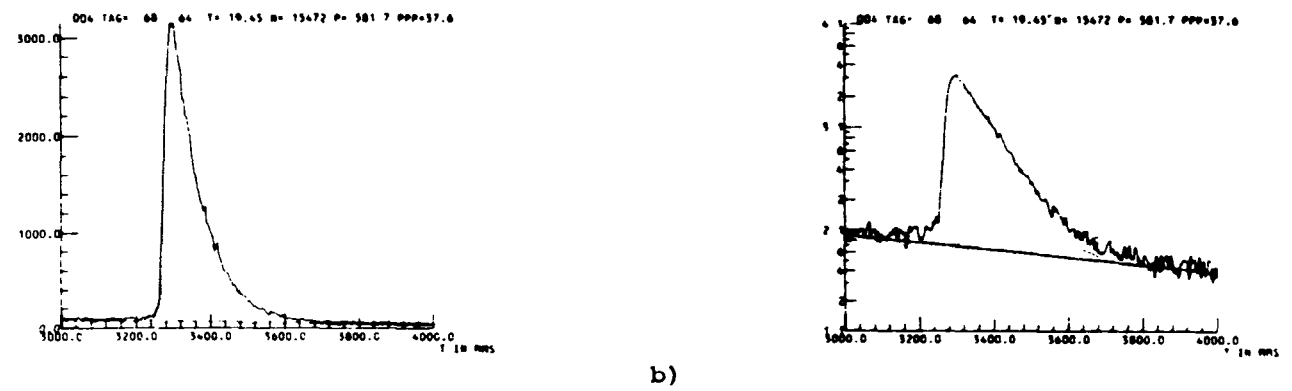

b)

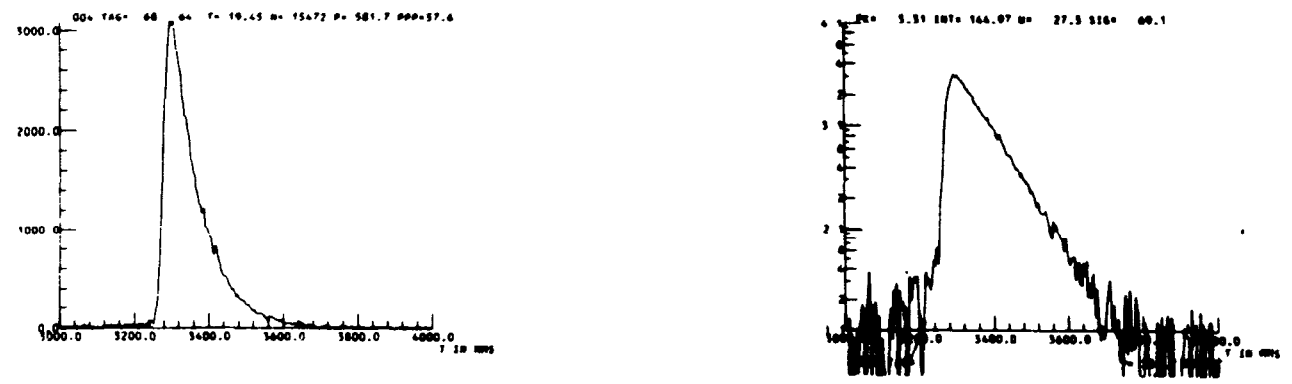

Fig. 14 a - f

Examples of background subtraction from the individual peaks in the spectrum of Fig. 13.

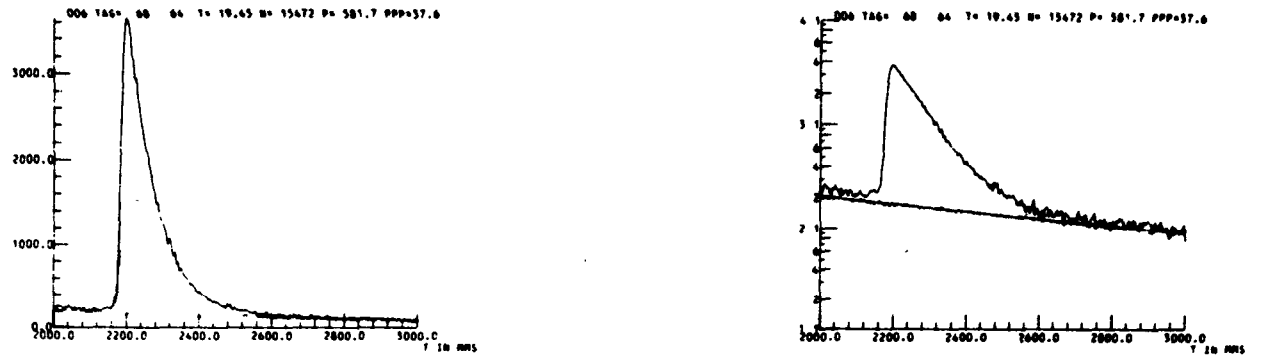

c)

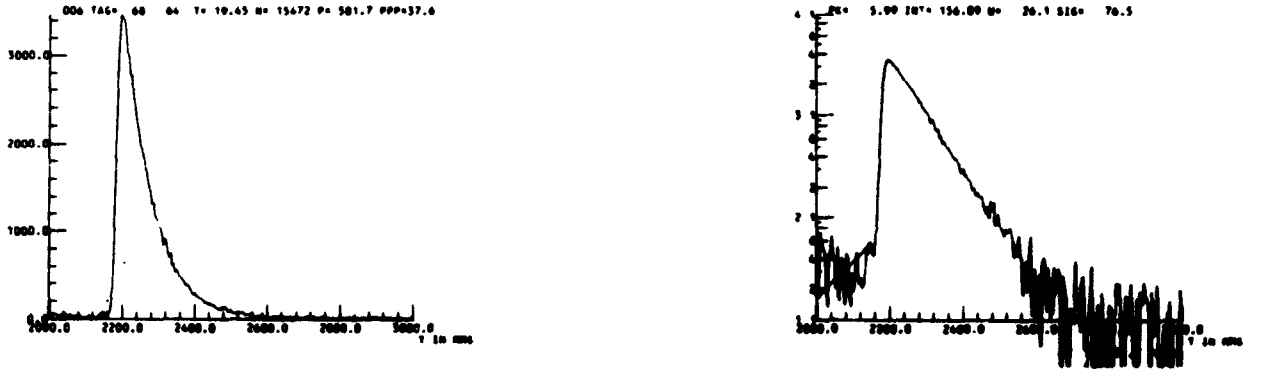

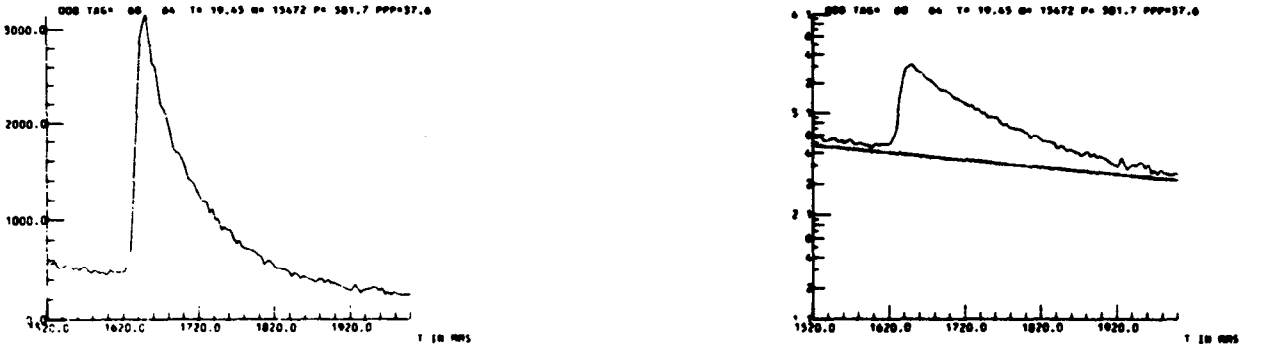

d)

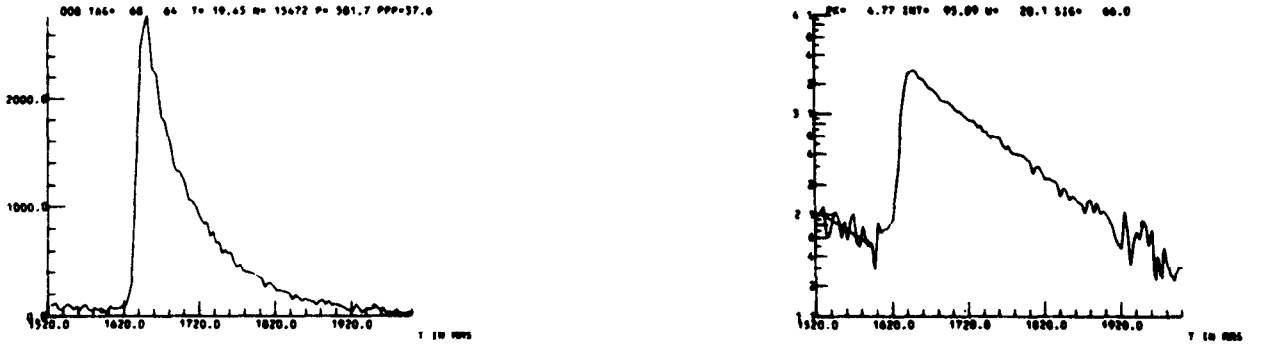

Fig. 14 a - f

Shown are the raw data in linear (upper left) and semilograrithmic representation (upper right) with the background level indicated and the same data with the background subtracted (lower right and left). Since the level of the background subtracted is scaled at the Cd-resonance region (see Fig. 13), there may remain some which is not part of the peak at the higher order reflections, which could be an overlap from the preceding peak.

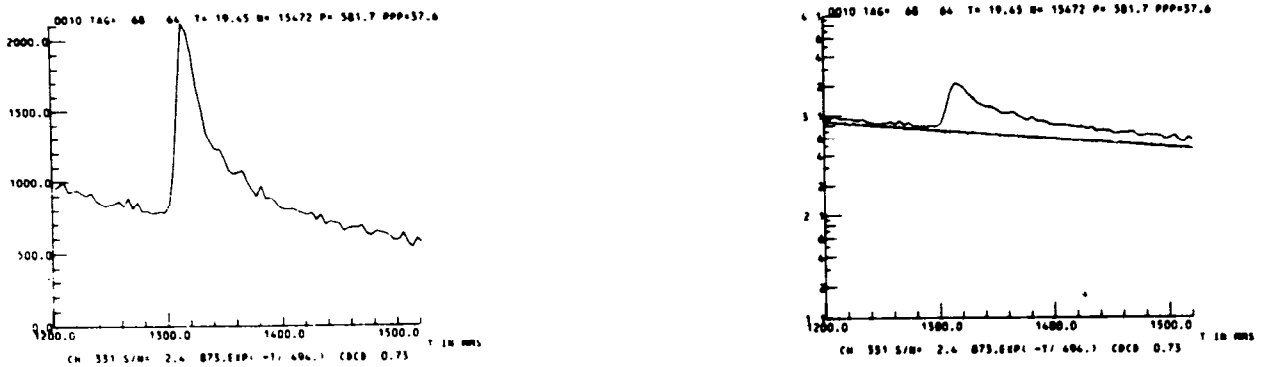

e)

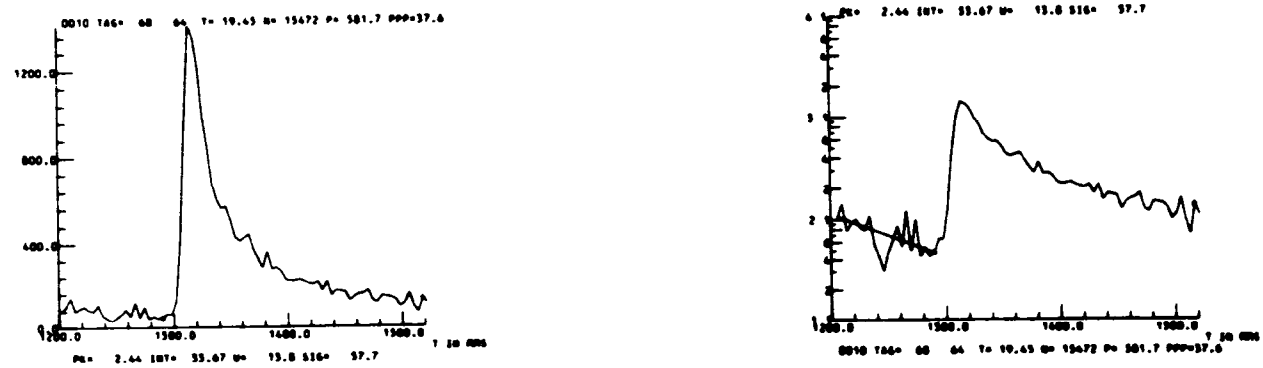

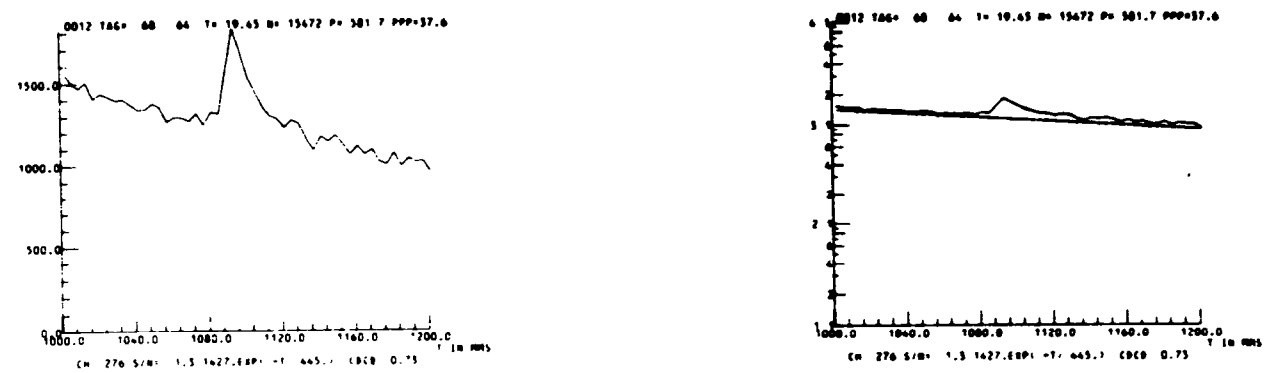

f)

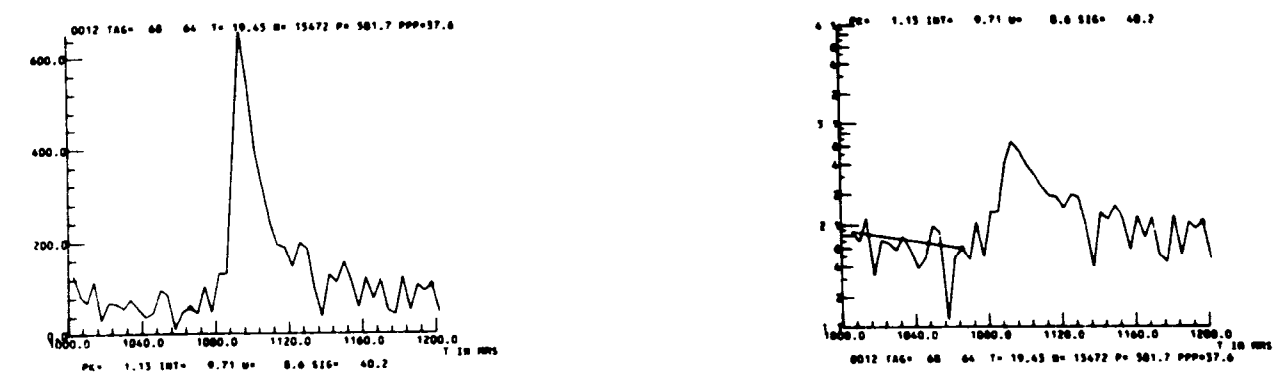

Fig. 14 a - f

One exponential decay function is sufficient to describe the 002, 004, 006 and also the 008 reflex. For the 0010 and 0012 reflex two decay constants are needed, but, at the same time, the statistical accuracy is getting poor.

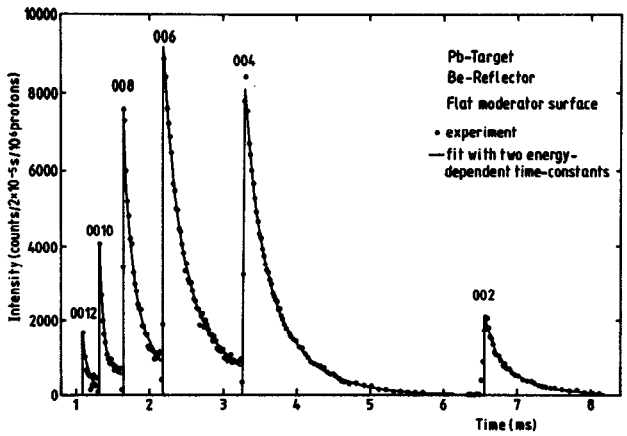

Fig.15 Reflection peaks of the graphite analyser for the flat surface moderator without decoupler and poison. The dates give the experimental data after the extrapolated overlap form the preceding peak has been substracted. The solid line is the result of a fit with two decay constants for each individual peak.

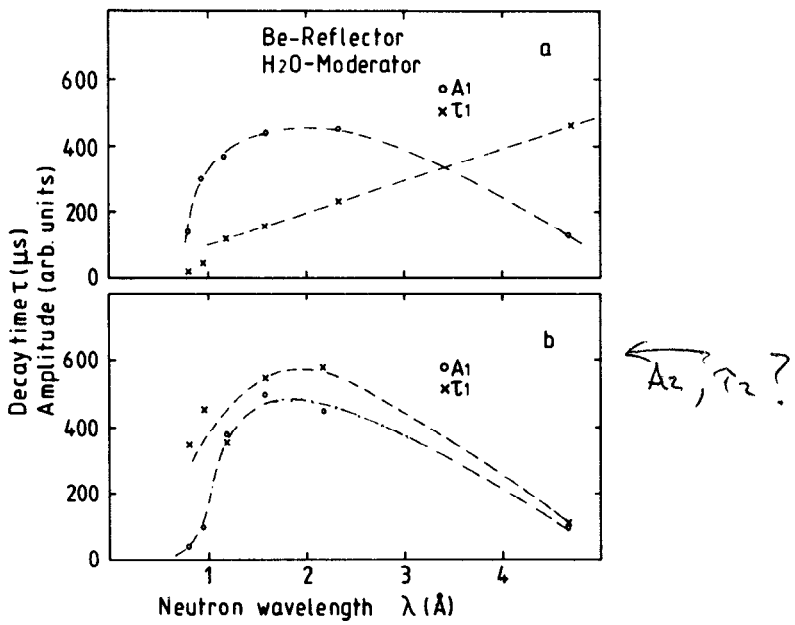

Fig. 16 Decay constants and corresponding amplitudes obtained from the fits of Fig. 15 as a function of neutron velocity.

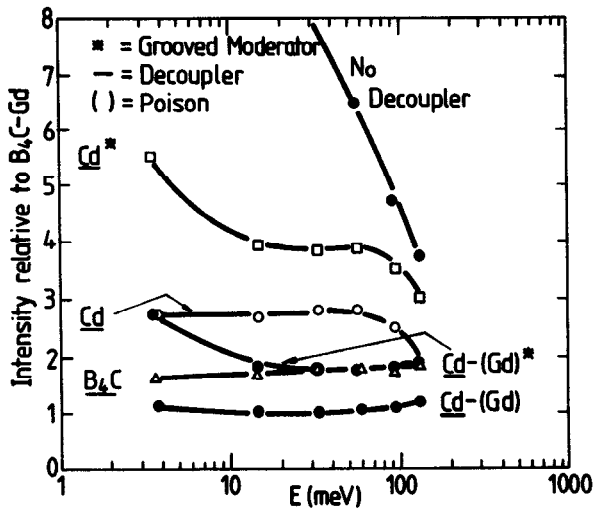

Fig. 17 Integrated intensities of the reflections for various combinations of decoupler and poison relative to the B_4C-decoupled-Gd poisoned case as a function of neutron energy.

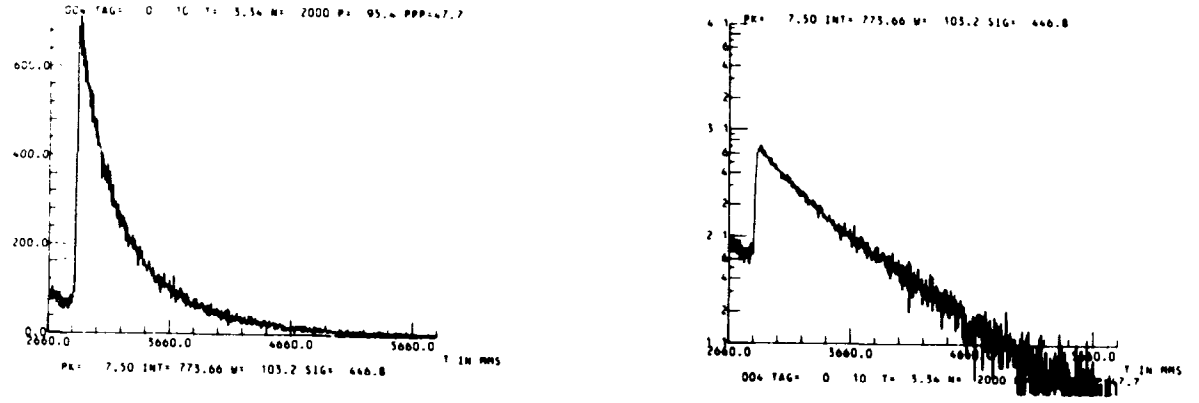

a)

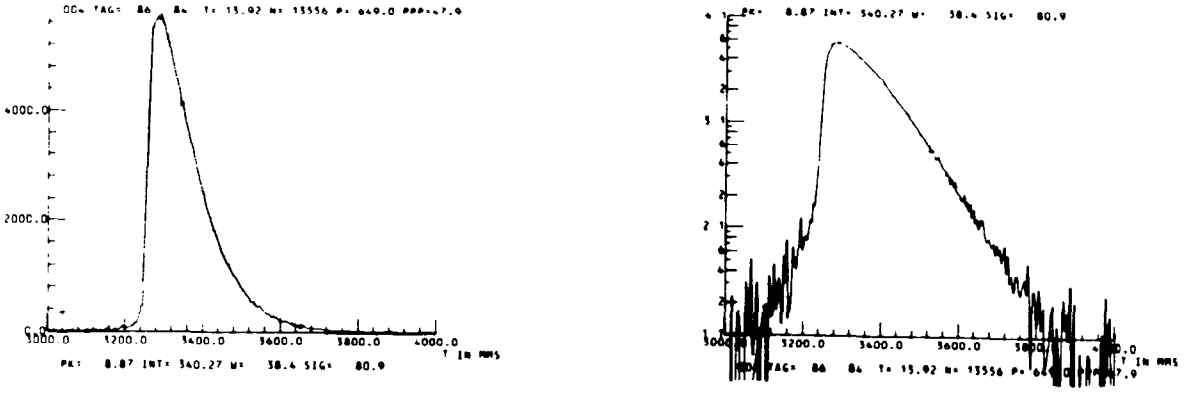

b)

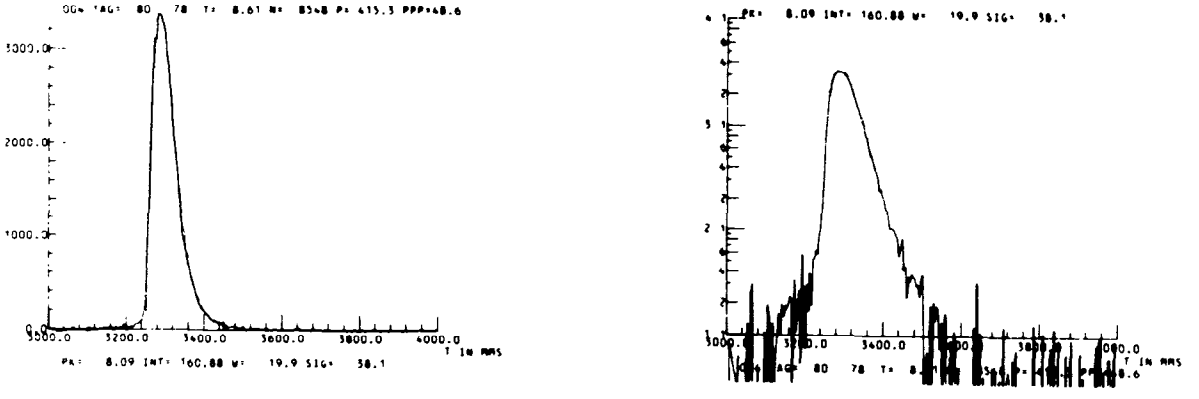

c)

Fig. 18 Comparison of the shapes of the 004-reflection (λ = 2.4 Å) for various combinations of moderator, decoupler and poison used

a) Grooved moderator, without decoupler and poison

b) Grooved moderator, Cd-decoupler

c) Grooved moderator, Cd-decoupler, Gd-poison.

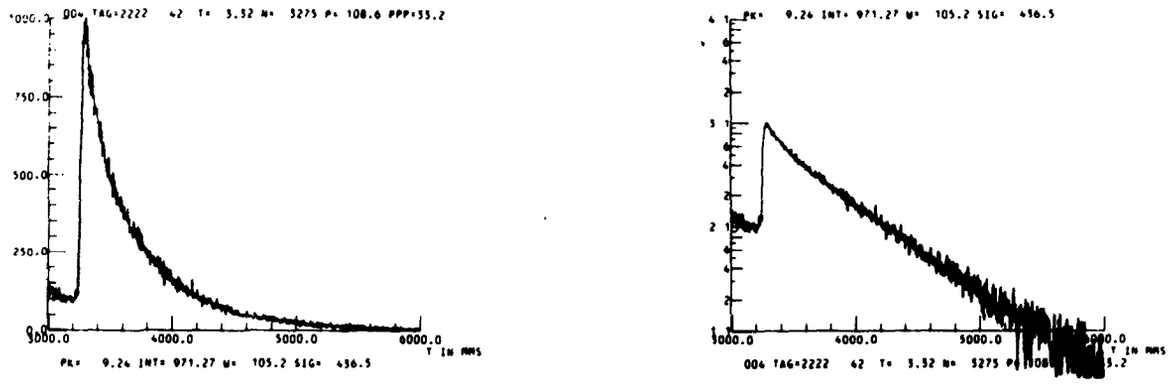

d)

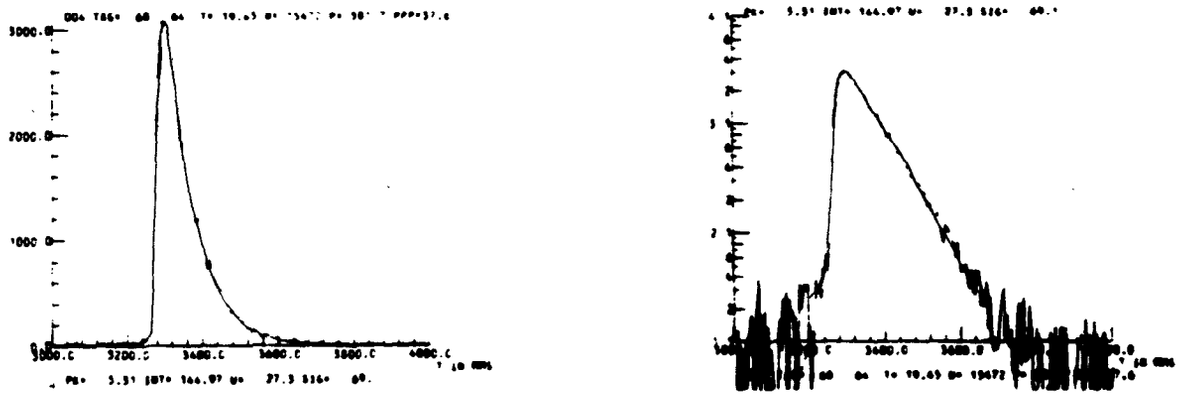

e)

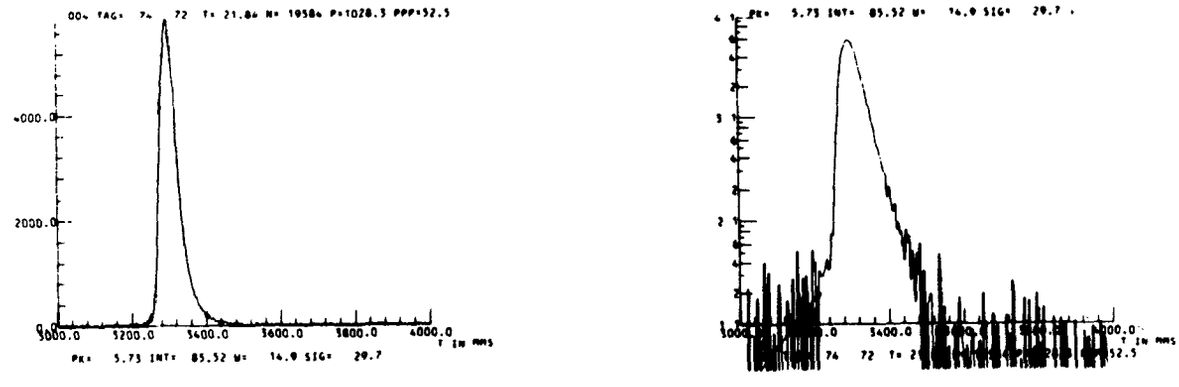

f)

Fig. 18 d) Flat moderator, without decoupler and poison

e) Flat moderator, B_4C-decoupler

f) Flat moderator, B_4C-decoupler, Gd-poison.

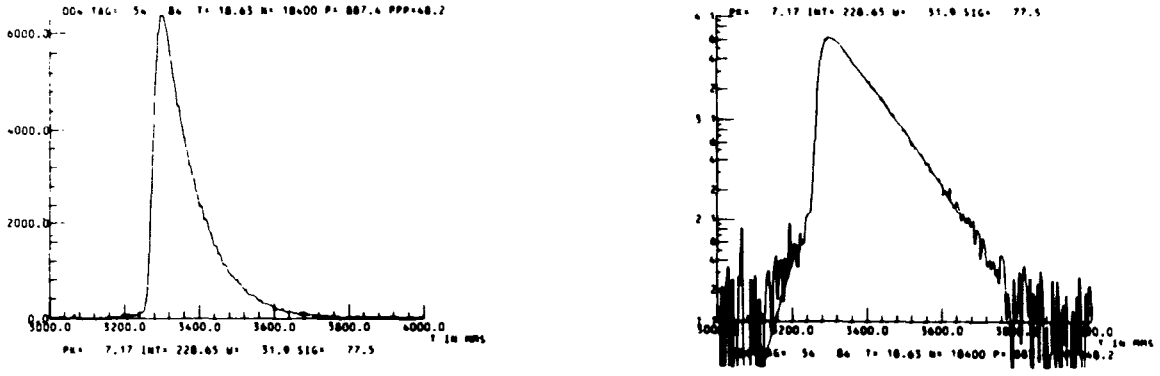

g)

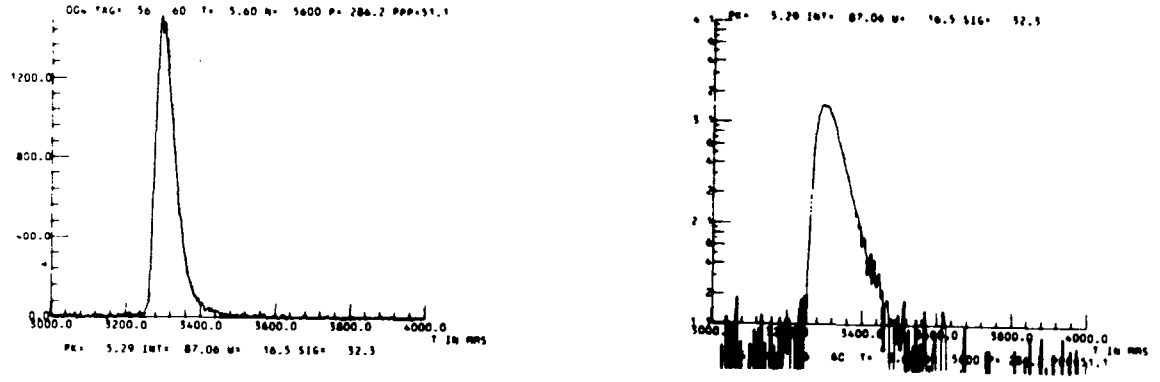

h)

Fig. 18 g) Flat moderator, Cd-decoupler

h) Flat moderator, Cd-decoupler, Gd-poison.